Engenharia Agrícola

ISSN: 1809-4430 (on-line)

www.engenhariaagricola.org.br

Scientific Paper
Doi: http://dx.doi.org/10.1590/1809-4430-Eng.Agric.v42n6e20220089/2022

DESIGN AND EXPERIMENT OF THE SEED DELIVERY DEVICE WITH A ROTATING BRUSH WHEEL FOR PRECISION SEEDER

Maojian Wei[1], Peisong Diao[1], Wenjun Wang[1*]

[1*]Corresponding author. School of Agricultural Engineering and Food Science, Shandong University of Technology/Zibo, China.
E-mail address: wjwang2016@163.com | ORCID ID: https://orcid.org/0000-0001-7101-3763

KEYWORDS

high speed precision seeder, seed collision, seed delivery device, U-shaped groove, flexible brush wheel.

ABSTRACT

In high speed seeding operation, the random collisions of seeds in the seed delivery tube seriously affect the seeding accuracy. In order to improve seeding uniformity and stability in high speed operation, the seed delivery device with a rotating brush wheel was designed, including U-shaped groove seed tube and flexible brush wheel. The optimization experiment was carried out by quadratic-regression rotatable orthogonal design method in JPS-12 seeding performance test bench. The three main factors were the rotate speed of seed metering device, the brush wheel diameter and the brush wheel speed. The evaluation indexes were the qualified rate of seeding spacing, miss seeding rate and coefficient of variation of seeding spacing. The results showed that the optimal parameters were rotate speed of seed metering device of 30 r/min, brush wheel diameter of 66 mm and brush wheel speed of 850 r/min. Finally, the verification experiment was carried out. The test results showed that the working performance of seed delivery device with a rotating brush wheel was obviously better than that of common seed delivery tube, especially at the forward speed of 15 km/h and above. The research provides a reference for the innovative design for a high speed precision seeder.

INTRODUCTION

Precision planting is an important development direction of modern agriculture, and is also one of the important measures to increase crop yield and decrease production cost. The technical core of precision planting is the precision seeding system, which is a series of devices providing seeds transport and freedom constraints in the process from the filling room to the seed furrow, including key technologies and devices of the single seed capture and the seed precise delivery (Jin et al., 2019; Yuan et al., 2018; Yang et al., 2016). Seed metering device, as the core component of single seed capture, is relatively mature at present and can basically realize single seed precision metering. Especially the pneumatic seed metering device, which has the characteristics of high single seed rate, lax requirements for seed size and strong vibration resistance, is widely used in the high-speed planter (Liao et al., 2020).

However, the development of seed precise delivery technology is relatively slow, that has become the main link affecting the seeds position in furrow, especially in the high speed operation (Kireev et al., 2019; Nielsen et al., 2018). In order to achieve precise control of seeds movement, scholars have carried out the researches on the active seed delivery technology, and some achievements have been used in seeders, such as brush-type seed delivery device (Wang et al., 2020a), flexible seed delivery belt (Lei et al., 2018; Kang et al., 2015), compartment-type seed delivery device (Liu, 2017). The active seed delivery device can effectively reduce the random collision in the process of seed transportation, and the seeding speed can reach 16 km/h (Chen & Zhong, 2012). These existing active seed delivery devices generally had the disadvantages of complex structure and long transmission distance, so they were not widely used in seeders.

[1] School of Agricultural Engineering and Food Science, Shandong University of Technology/Zibo, China.

Area Editor: Francisco Scinocca
Received in: 6-4-2022
Accepted in: 10-25-2022

At present, the passive seed guidance and transport technology (seed delivery tube) was used by most seeders, and a lot of researches were mainly focused on the development of seed delivery tube (Yu et al., 2014) found that the motion track of seeds leaving the seed metering device at a certain initial speed was a spatial parabola. Based on the parabola, the seed delivery tube was designed to avoid changing the orderly movement of seeds due to the violent collision. (Liu et al., 2016) used the discrete element method to simulate the falling process of seeds in the seed delivery tube, and found that when the operating speed was 1.389 m/s, the optimal height of the seed delivery tube was 500 mm.(Zhao et al., 2018) designed the V-groove dialing round type seed delivery device to improve the uniformity and stability of seed delivery, and the test results showed that when the rotate speed of seed disk was 45 r/min, the coefficient of variation of seeding spacing was 30.55% higher than that of the common seed tube.

But due to the limitations of the seed delivery tube itself, the seeds will collide with the tube wall in the falling process and change their orderly movement, so that seeds can not accurately fall into the designated point of the seed furrow. The collision between the seed and the tube wall directly affected the uniformity of seeding spacing, the straightness of seed belt and consistency of seeding depth (Li et al., 2020).

With the increase of working speed, the variation of seeds position will further increase, and the accuracy of seeds implantation will also significantly reduce, which eventually fail to meet the agronomic requirements. Therefore, the seed delivery device with a rotating brush wheel was designed to improve the motion track of seeds in the seed delivery tube. Through theoretical analysis and optimization experiment, the main structural parameters and effects of each factor on seed transport performance was determined. Finally, the verification experiment was carried out to prove the rationality of the parameters. This study provides theoretical methods and technical references for the development of the high-speed precision planting technology.

MATERIAL AND METHODS

Overall structure and working principle of seed delivery device with a rotating brush wheel

As shown in Figure 1, the seed delivery device with a rotating brush wheel is mainly composed of U-shaped groove seed tube, flexible brush wheel, stepping motor and its control system. The U-shaped groove seed tube was 3D printed with photosensitive transparent resin material and its seed guide curve adopted the combination of "inclined straight line + fastest descent curve" to reduce the movement time of seeds in the tube. The cross section of the seed tube was designed in the shape of a U-shaped groove, which was based on the overall size of soybean seeds, forming a U-shaped slide track together with the seed guide curve. The flexible brush wheel was made of nylon material and driven by a stepping motor. The motor control system could adjust the rotate speed of the brush wheel in real time. The seeds leaving the seed metering device moved closely to the U-shaped slide track under the restraint and guidance of the flexible brush wheel.

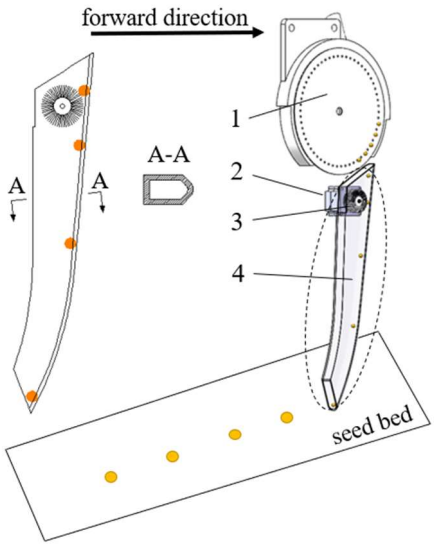

Note: 1. Seed metering device; 2. Stepping motor and its control system; 3. Flexible brush wheel; 4. U-shaped groove seed tube.

FIGURE 1. Overall structure of seed delivery device with a rotating brush wheel.

The seed delivery device with a rotating brush wheel was installed at the outlet of a seed metering device. Take air-suction seed metering device as the carrier, the seed sucking plate rotates to realize seed picking, carrying, cleaning and throwing. Below the seed metering device, the flexible brush wheel is driven by a stepping motor and rotates at a fixed proportional rotate speed. The seed leaving the seed metering device will fall into the clearance between the brush wheel and the tube wall. The track and speed of the seed is adjusted under the restraint and guidance of the brush wheel, ensuring that the seed is close to the inner wall of the seed guide curve. Then the seed is guided into the U-shaped slide track, which makes the seed slide stably under itself own gravity. The constraint and guidance of the seed guide curve and U-shaped groove avoid the collision and deviation of seeds in the seed tube, realizing the stable and orderly seed transport, and improving the uniformity and stability of the seeding operation.

Design of U-shaped groove seed tube

The main structure of U-shaped groove seed tube includes two parts: seed guide curve and U-shaped groove. In order to reduce the movement time of seeds in tube and improve the smoothness of the seed slide, the seed guide curve adopted the combination of "inclined straight line + fastest descent curve". As shown in Figure 2, the area I was the brush wheel restraint stage (inclined straight line) and the area II was the guide curve stage (fastest descent curve). Taking the inlet of seed tube as the coordinate origin O, the forward direction of the machine as X-axis, the vertical downward direction as Y-axis, and the rectangular coordinate system XOY was established. Through the kinematic and dynamic analysis of seeds in the tube (Zhao et al., 2018), the equation of seed guide curve was obtained as $Y = -0.02X^2+3.9X$.

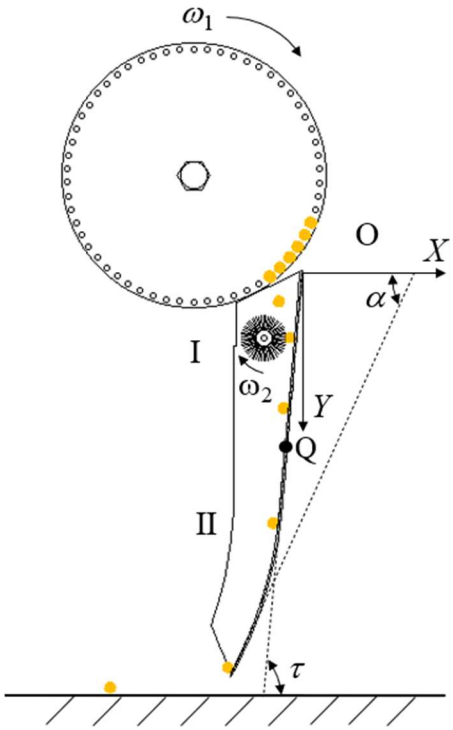

Note: Q is the starting point of the fastest descent curve; τ is the angle of the inclined straight line; α is the tangent inclination of the downgrade line.

FIGURE 2. U-shaped groove seed tube.

In order to make the seeds move close to the center line of the seed tube wall, the U-shaped groove of the seed tube was designed, as shown in Figure 3. The bottom of the U-shaped groove cross section adopted the combination of symmetrical straight line and circular arc. Due to the symmetrical U-shaped groove cross section, the seed eventually would slide along the center line of the seed tube wall under the constraint of the U-shaped groove during the sliding process, reducing the lateral movement of seeds in the seed tube, effectively reducing the lateral deviation of the seed position in furrow.

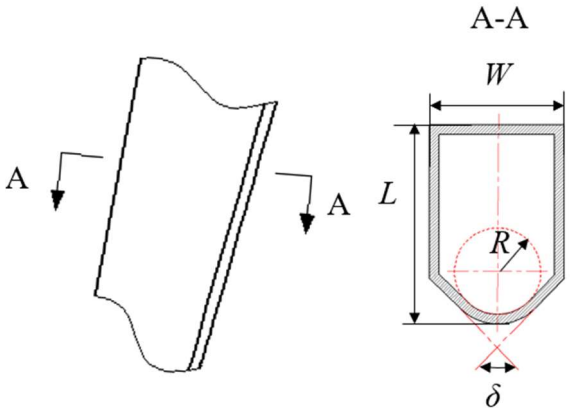

FIGURE 3. Cross section of U-shaped groove seed tube.

The structure parameter of U-shaped groove directly affected the movement accuracy of seeds. If the size of U-shaped groove was too large, the constraint on seeds would be reduced, increasing lateral deviation and collision. Conversely, the sliding resistance of seeds would be increased, reducing the smoothness of seeds slide. In order to improve the adaptability of the U-shaped groove to the seed size, the structural parameter design was conducted with soybean seeds as the research object. Three soybean varieties (Zhonghuang 39, Yimengshan and Heilongjiang) commonly planted in northern China were selected in the study. Five hundred soybean seeds were randomly selected and their overall dimensions (length, width and thickness) were measured with a caliper with 0.01 mm accuracy. The measurement results of soybean size showed that the length (l) was 6.5-8.2 mm, the width (w) was 5.8-7.0 mm, the thickness (t) was 4.2-6.9 mm. The basic structural parameters of U-shaped groove should follow the following design principles (Wang et al., 2017):

$$\begin{cases} 7.2\bar{l} \geq L \geq 6.3\bar{l} \\ 4.1\overline{w} \geq W \geq 3.4\overline{w} \end{cases} \quad (1)$$

in which:

$\bar{l}$ -the average length of seeds, mm,

$\overline{w}$ -the average width of seeds, mm.

According to [eq. (1)], the structural sizes of the U-shaped groove section were calculated: height L=58 mm, width W=24 mm.

The angle δ of U-shaped groove reflected the constraint ability of the seed tube to seeds. If the angle δ was too small, it was easy to cause the seeds to get stuck in the U-shaped groove, affecting the smoothness of seed slide. Conversely, the ability of seeds to return to the equilibrium position (center line of the seed tube) would be reduced in the process of seeds slide, affecting the seed position accuracy. Therefore, considering the stability of seeds sliding motion comprehensively, the angle of U-shaped groove was designed as δ =90°. The bottom of the U-shaped groove was a circular arc, which was tangent to the symmetrical straight line on both sides of the angle δ. In order to ensure seeds slide along the seed tube wall and avoid getting seeds stuck in the U-shaped groove, the diameter of the circular arc should be larger than the maximum size of soybean seeds. Referring to the maximum size of soybean seeds (8.2 mm), the diameter of the circular arc was designed as 9 mm.

Design of flexible brush wheel

The physical properties of flexible brush wheel directly affected the seed guiding performance, so it was very important to select an appropriate brush material. Nylon material was characterized by high toughness, good wear resistance and strong resilience (Hou et al., 2020). Therefore, the flexible brush wheel adopted nylon material. After leaving the seed metering device, the seed made a parabolic motion under the action of its own gravity and the reaction force of the stopper, finally falling into the clearance between the brush wheel and the tube wall, as shown in Figure 4. In the following analysis, it was assumed that there was no energy loss when the seed impacted the stopper, and the reflection law was followed.

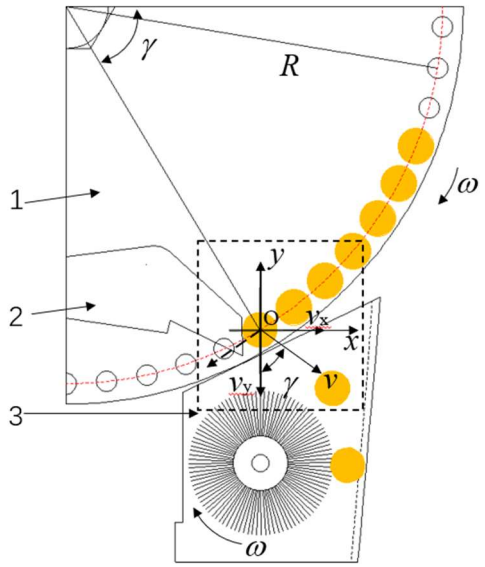

Note: 1. Seed metering device; 2. Stopper; 3. U-shaped groove seed tube.

FIGURE 4. Analysis of seeds throwing process.

Taking the seed that was about to leave the sucking plate as the coordinate origin *O*, the forward direction of the machine as *x*-axis, the vertical downward direction as *y*-axis, and the rectangular coordinate system *xOy* was established. The kinematic equation of the seed was obtained as follows.

$$\begin{cases} x = v_x t \\ y = v_y t + \dfrac{1}{2} g t^2 \\ v_x = v \sin\gamma \\ v_y = v \cos\gamma \\ v = \dfrac{n\pi R}{30} \end{cases} \tag{2}$$

in which:

v-the seed velocity, mm/s;

v_x-the horizontal velocity of the seed, mm/s;

v_y-the vertical velocity of the seed, mm/s;

γ-the seed throwing angle, (°);

t -the time after the seed throwing, s,

R-the radius of seed sucking plate, mm.

According to [eq. (2)], the following equation was derived.

$$\begin{cases} x = \dfrac{n\pi R \sin\gamma}{30} t \\ y = \dfrac{n\pi R \cos\gamma}{30} t + \dfrac{1}{2} g t^2 \end{cases} \tag{3}$$

The mounting height of flexible brush wheel was set as *y*=50 mm, the seed throwing angle was set as *γ*=47°, the seed plate radius was set as *R*=123 mm, the rotate speed range of seed metering device was set as *n*=30-50 r/min. The above data were put into [eq. (3)] to obtain and the minimum horizontal displacement distance of the seed thrown from metering device was *x*=50 mm.

After leaving the seed metering device, the seed would fall into the clearance between the brush wheel and the tube wall. Under the action of rotating brush wheel, the motion state of the seed was changed. Therefore, it was necessary to carry out dynamic analysis of the seed in the clearance between the brush wheel and the tube wall, which was shown in Figure 5.

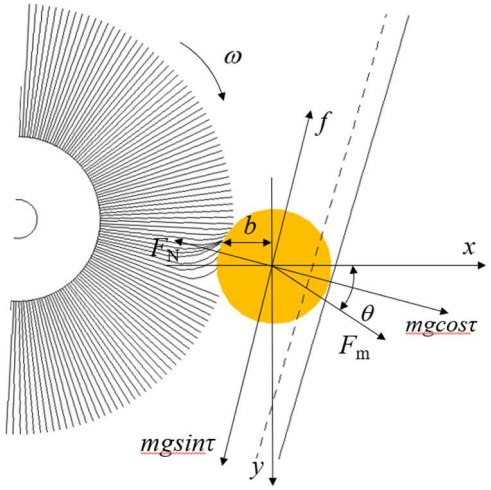

FIGURE 5. Force analysis of the seed in the clearance between the brush wheel and the tube wall.

From Figure 5, the following equation was obtained.

$$\begin{cases} F_m \sin\theta + mg - f_y - F_N \cos\tau = 0 \\ F_m \cos\theta + f_x - F_N \sin\tau = 0 \\ f = \mu F_N \end{cases} \tag{4}$$

in which:

F_m-the force acted on the seed by brush silk, N;

θ-the Angle between F_m and *x*-axis, (°);

f_x-the *x*-axis component of friction force *f*, N;

f_y -the *y*-axis component of friction force *f*, N;

μ-the friction coefficient between the seed and brush silk;

F_N-the supporting force of the tube wall on the seed, N;

m-the seed mass, g,

τ-the angle of the inclined straight line, (°).

In order to ensure that the seeds can slide closely to the tube wall, the torque applied by the brush wheel to the seed should meet [eq. (5).

$$F_m b\sin\theta - F_m\sqrt{r^2-b^2}\cos\theta < (\mu-\sin\tau)mgr\cos\left[\arcsin\left(\frac{b}{r}\right)-\tau\right] \tag{5}$$

in which:

r-the seed radius, mm;

b-the distance from the contact point to the seed center in the *x*-axis direction, mm.

To simplify the analysis, the brush silk treated as a cantilever beam, as shown in Figure 6. The left end of the cantilever beam was fixed constraint, and the right end was free, subject to a vertical upward force *F* (reaction force from the seed). Under the force *F*, the brush silk deformed to the position of dotted line in Figure 6. Take the left end of the brush silk as the center of the circle to establish xOy coordinate system, so the deflection curve and bending angle function could be expressed as $f(x)$ and $\beta(x)$.

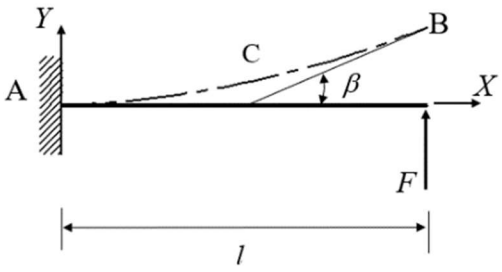

FIGURE 6. Force analysis of the brush silk.

The relationship between the deflection curve $f(x)$ and the bending angle function $\beta(x)$ was as follows.

$$f'(x) = \tan(\beta(x)) \tag{6}$$

Take the derivative of [eq. (6)] with respect to *x*, and obtain the following equation.

$$f''(x) = \sec^2[\beta(x)]\frac{d\beta(x)}{dx} \tag{7}$$

The curvature radius, bending moment and deflection curve should satisfy the following equation.

$$\frac{1}{\rho(x)} = \frac{M(x)}{EI} \tag{8}$$

$$M(x) = Fl \tag{9}$$

$$\frac{1}{\rho(x)} = \pm\frac{f''(x)}{\left\{1+[f'(x)]^2\right\}^{\frac{3}{2}}} \tag{10}$$

in which:

$\rho(x)$-the curvature radius, mm;

$M(x)$-the bending moment, kN·m;

E-the elastic modulus, GPa;

I-the inertia moment, mm^4;

F-the reaction force from the seed, N,

l-the brush silk length, mm.

Bring eqs (6) and (7) into [eq. (10)], and obtain the following equation.

$$\frac{1}{\rho(x)} = \pm\cos\beta(x)\frac{d\beta(x)}{dx} \tag{11}$$

Combine eqs (8), (9) and (11) to obtain the following equation.

$$\frac{Fl}{EI}dx = \pm\cos\beta(x)\,d\beta(x) \tag{12}$$

Integrate [eq. (12)] to obtain the following equation.

$$\beta(x) = \pm\arcsin\left(\int\frac{Fl}{EI}dx\right) \tag{13}$$

Bring [eq. (13)] into [eq. (5)], and obtain [eq. (14)].

$$F_m < \frac{(\mu-\sin\tau)mgr\cos\left[\arcsin\left(\frac{b}{r}\right)-\tau\right]}{b\sin\left[\pm\arcsin\left(\int\frac{Fl}{EI}dx\right)\right]+\sqrt{r^2-b^2}\cos\left[\pm\arcsin\left(\int\frac{Fl}{EI}dx\right)\right]} \tag{14}$$

It is assumed that there was no mechanical energy loss in the system during the collision between the brush silk and the seed, the energy transfer should satisfy the following equation after time Δt.

$$\frac{1}{2}J_0\omega_0^2-\frac{1}{2}J_1\omega_1^2=\frac{1}{2}m\left(v_1^2-v_0^2\right)+W_{F_m} \quad (15)$$

in which:

J_0-the moment of inertia of the brush silk, kg·m^2;

J_1-the moment of inertia of the brush silk after the time Δt, kg·m^2;

ω_0-the angular velocity of the brush silk at the moment of collision, rad/s;

ω_1-the angular velocity of the brush silk after the time Δt, rad/s;

v_0-the velocity of the seed at the moment of collision, m/s;

v_1-the velocity of the seed after the time Δt, m/s;

W_{Fm}-the mechanical work done by F_m in the time Δt.

According to [eq. (14)], the force F_m acted on the seed by brush silk was related to the brush silk length l, the seed radius r and the position of the contact point b. The seed radius r and the position of the contact point b were uncontrollable, and the brush silk length l determined directly the brush wheel diameter, so the brush wheel diameter became one of the main impact factors that can be controlled. According to [eq. (15)], the force F_m was also directly related to the rotate speed of the brush wheel and the seed speed. Among them, the initial speed of the seed was determined by the rotate speed of seed metering device. So the rotate speed of the brush wheel and the rotate speed of seed metering device were also the main impact factors.

Therefore, the brush wheel diameter, rotate speed of seed metering device and brush wheel speed would be selected as factors in the following optimization experiment.

Experiment conditions and equipment

The parameter optimization experiment and validation experiment was carried out respectively in the intelligence agricultural machinery laboratory of Shandong University of Science and Technology. The main experimental equipment included air-suction seed metering device, JPS-12 seeding performance test bench (Figure 7), high-speed camera (A5031M/CU815, Dahua, China), computer, stepping motor (57EBP143ALC-TFC, Time Brilliant, China) and its control system (Figure 8). Before the experiment, the air-suction seed metering device was fixed on the frame of JPS-12 seeding performance test bench, and the seed delivery device with a rotating brush wheel was installed below the seed throwing port of the metering device. During the operation, the image acquisition and data processing system of the test bench and high-speed camera system were used to accurately measure the seeding performance indexes.

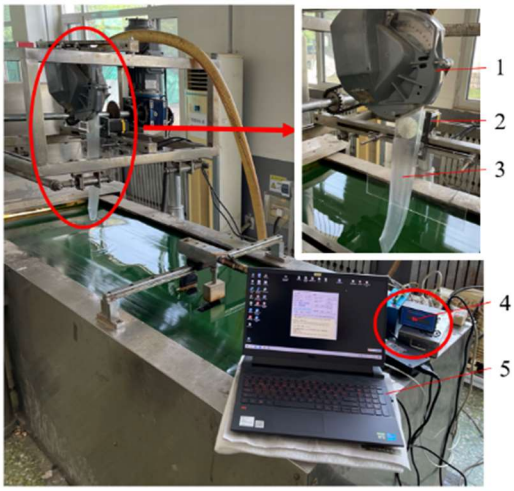

Note: 1. Air-suction seed metering device; 2. Stepping motor; 3. U-shaped groove seed tube; 4. Motor control system; 5. Computer

FIGURE 7. Test bench for measuring seeding performance.

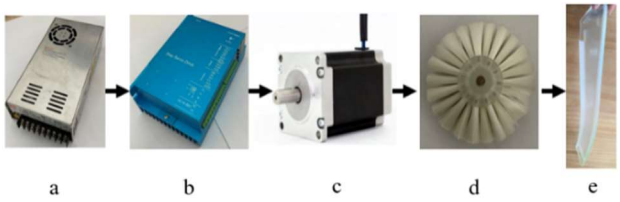

Note: a. DC power supply; b. Motor driver; c. Stepping motor; d. Flexible brush wheel; e. U-shaped groove seed tube

FIGURE 8. Composition and installation of motor control system.

Parameter optimization experiment

According to the theoretical analysis, the main factors affecting the seeding performance were the rotate speed of seed metering device, the brush wheel diameter and the brush wheel speed. In order to determine the optimal parameters of seed delivery device with a rotating brush wheel, the optimization experiment was carried out by quadratic-regression rotatable orthogonal design method. Each group was repeated for 3 times, and the average value of data was taken as the experiment result. The experimental factors and levels are shown in Table 1, and the design scheme is shown in Table 2.

TABLE 1. Experimental factors and levels.

Code	Rotate speed of seed metering device/ (r·min^{-1})	Brush wheel diameter/mm	Brush wheel speed/ (r·min^{-1})
1.682	100	66	850
1	85	62	789
0	65	58	700
-1	45	54	610
-1.682	30	50	550

According to "GB/T 6973-2005 Testing methods of single seed drills (precision drills)" in China, the qualified rate of seeding spacing (Q), miss seeding rate (M) and coefficient of variation of seeding spacing (C) were selected as evaluation indexes.

$$\begin{cases} Q = \dfrac{n_0}{N} \times 100\% \\ M = \dfrac{n_1}{N} \times 100\% \\ C = \sqrt{\dfrac{\sum (x - \bar{x})^2}{(n'-1)\bar{x}^2}} \times 100\% \end{cases} \quad (16)$$

in which:

n_0-the number of seeds with qualified seeding spacing, %;

n_1-the number of seeds with miss seeding, %;

N-the theoretical seed number;

n'-the number of seeds measured;

x-the theoretical seeding spacing, mm,

$\bar{x}$ -the mean of actual seeding spacing, mm.

Validation experiment

In order to verify the rationality of the optimal parameters and analyze the stability of the device, the validation experiment was carried out. In addition to the use of JPS-12 seeding performance test bench, a high-speed camera was also used to collect the movement state of seeds leaving seed meter device.

The performance of seed delivery device with a rotating brush wheel and common seed delivery tube (Figure 9) were compared under different working speeds. The evaluation indexes were qualified rate of seeding spacing, coefficient of variation of seeding spacing and lateral deviation. The qualified rate of seeding spacing, coefficient of variation of seeding spacing were obtained by [eq. (16)]. The measurement method of lateral deviation was as follows: Based on the center line of the theoretical seeds belt, the lateral distances of seeds relative to the center line were measured. The data of 30 consecutive seeds was recorded each time, repeated 3 times, and the average value was calculated (Wang et al., 2020b).

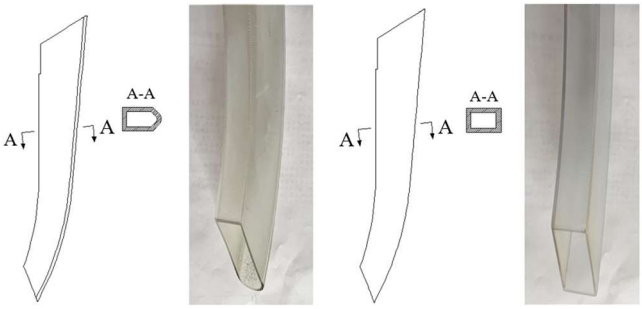

FIGURE 9. Common seed delivery tube and seed delivery device with a rotating brush wheel.

RESULTS AND DISCUSSION

Parameter optimization experiment

The results of parameter optimization experiment are showed shown in Table 2.

TABLE 2. Design scheme and results.

No.	Rotate speed of seed metering device X_1	Brush wheel diameter X_2	Brush wheel speed X_3	Qualified rate of seeding spacing Q/%	Miss seeding rate M/%	Coefficient of variation of seeding spacing C/%
1	-1	-1	-1	95.7	2.15	20.08
2	1	-1	-1	85.71	6.22	22.06
3	-1	1	-1	94.9	3.06	19.65
4	1	1	-1	84.55	7.07	25.7
5	-1	1	1	96.12	0.2	18.25
6	1	-1	1	87.25	4.9	25.12
7	-1	1	1	96.12	0.5	15.36
8	1	1	1	86.41	4.85	25.9
9	-1.682	0	0	93.97	0.96	16.4
10	1.682	0	0	78.3	8.72	26.0
11	0	-1.682	0	97.0	1.0	20.18
12	0	1.682	0	95.51	2.2	22.17
13	0	0	-1.682	89.58	6.25	22.76
14	0	0	1.682	92.08	2.19	21.23
15	0	0	0	95.82	2.04	21.33
16	0	0	0	94.0	2.0	20.74
17	0	0	0	93.66	1.99	20.28
18	0	0	0	95.92	1.72	20.86
19	0	0	0	93.26	2.02	21.44
20	0	0	0	94.06	1.98	19.94
21	0	0	0	95.0	2.0	21.75
22	0	0	0	94.95	2.02	21.96
23	0	0	0	95.7	2.23	19.96

Design-expert 10.0 software was used for multiple regression fitting of the experiment data (Liu, 2017), and the regression model of each evaluation index is shown in eqs (17)-(19). The variance analysis of regression equations for each evaluation index is shown in Table 3. From the Table 3, the P values of terms X_1 and X_3 were all less than 0.05 for each evaluation index, indicating the impacts are significant. However, the P values of the item X_2 is less than 0.05 only for the miss seeding rate, and greater than 0.05 for the other two indexes. So the item X_2 had a significant impact on the miss seeding rate, but has no significant effect on the other two indexes.

$$Q = 94.72 - 4.78X_1 - 0.39X_2 + 0.68X_3 - 3.04X_1^2 + 0.54X_2^2 - 1.38X_3^2 \quad (17)$$

$$M = 2.01 + 2.21X_1 + 0.29X_2 - 1.09X_3 + 0.12X_1X_3 - 0.19X_2X_3 + 0.99X_1^2 - 0.15X_2^2 + 0.78X_3^2 \quad (18)$$

$$C = 20.92 + 3.05X_1 + 0.33X_2 - 0.4X_3 + 0.97X_1X_2 + 1.17X_1X_3 - 0.67X_2X_3 + 0.39X_3^2 \quad (19)$$

TABLE 3. Variance analysis.

Source	Qualified rate of seeding spacing	Miss seeding rate	Coefficient of variation of seeding spacing
X_1	<0.0001**	<0.0001**	<0.0001**
X_2	0.0992	<0.0001**	0.0904
X_3	0.0086**	<0.0001**	0.0436*
X_1X_2	0.6086	0.4006	0.0011**
X_1X_3	0.4553	0.0604	0.0002**
X_2X_3	0.6325	0.0070**	0.0134*
X_1^2	<0.0001**	<0.0001**	0.5353
X_2^2	0.0191*	0.0032**	0.5697
X_3^2	<0.0001**	<0.0001**	0.0359*

Note: P ≤0.01, ** means extremely significant; 0.01 < P < 0.05, * means significant; P > 0.05, means no significant.

In order to analyze the relationship between experimental factors and indexes more intuitively, the response surfaces were drawn in Design-Expert 10.0, as shown in Figure 10 and 11.

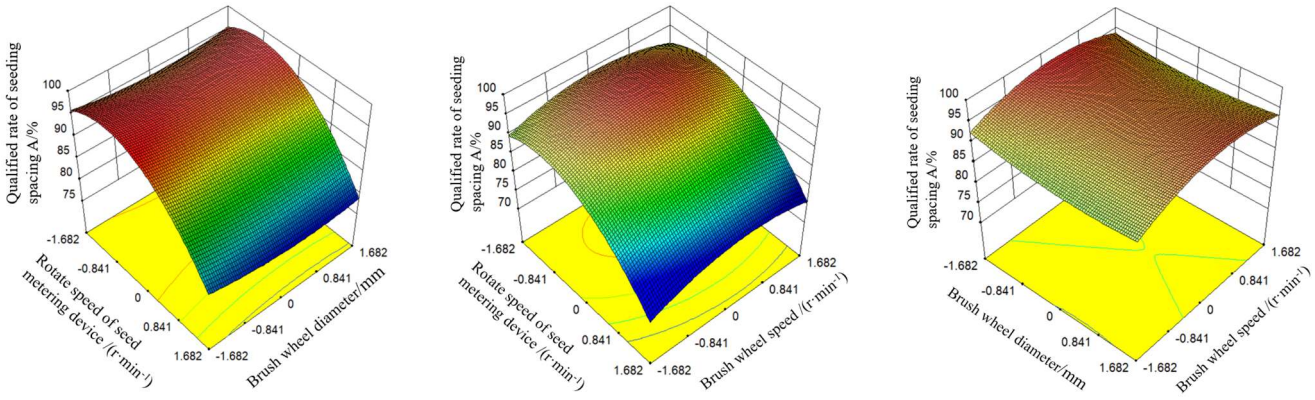

(a) Q=f（X_1，X_2，0） (b) Q=f（X_1，0，X_3） (c) Q=f（0，X_2，X_3）

FIGURE 10. Effect of various factors on the qualified rate of seeding spacing.

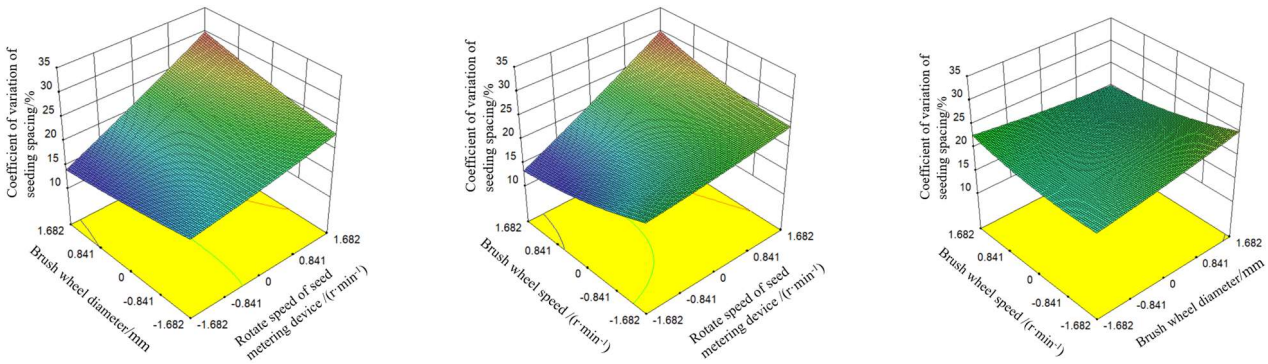

(a) C=f（X_1，X_2，0） (b) C=f（X_1，0，X_3） (c) C=f（0，X_2，X_3）

FIGURE 11. Effects of various factor on the coefficient of variation of seeding spacing.

As shown in Figure 10a, with the increase of brush wheel diameter, the qualified rate of seeding spacing fluctuated slightly, so the impact was not significant. With the increase of rotate speed of seed metering device, the qualified rate of seeding spacing increased at first and then decreased, and the amplitude was obvious. So the rotate speed of seed metering device had a significant impact on the qualified rate of seeding spacing. From Figure 10b, with the increase of brush wheel speed, the qualified rate of seeding spacing increased at first and then decreased. With the increase of rotate speed of seed metering device, the qualified rate of seeding spacing changed steadily at first and then decreased sharply. Therefore, the rotate speed of seed metering device and brush wheel speed both had a significant impact on the qualified rate of seeding spacing. From Figure 10c, with the increase of brush wheel speed, the qualified rate of seeding spacing increased at first and then decreased. With the increase of brush wheel diameter, the qualified rate of seeding spacing had no significant change.

As shown in Figure 11a, with the increase of brush wheel diameter, the coefficient of variation of seeding spacing decreased gradually when the rotate speed of seed metering device was small, and increased gradually when the rotate speed of seed metering device was large. But the change was small, so the effect of brush wheel diameter was not significant. With the increase of rotate speed of seed metering device, the coefficient of variation of seeding spacing increased rapidly, so the effect of the rotate speed of seed metering device was significant. From Figure 11b, with the increase of brush wheel speed or rotate speed of seed metering device, the coefficient of variation of seeding spacing changed obviously. So the brush wheel speed and rotate speed of seed metering device both had a significant impact on the coefficient of variation of seeding spacing. From Figure 11c, the effect of brush wheel speed on the coefficient of variation of seeding spacing was greater than that of brush wheel diameter. From Figure 11a-c, the interaction of any two of the three factors had a significant impact on the coefficient of variation of seeding spacing.

In order to obtain the optimal parameters, the optimization objectives of the highest qualified rate of seeding spacing, lowest coefficient of variation of seeding spacing and boundary conditions of each factor provide the objective functions and constraints, as shown in [eq. (20)]. The optimization module of Design-Expert was used to solve the regression model. The results showed that the optimal parameters were rotate speed of seed metering device of 30 r/min, brush wheel diameter of 66 mm and brush wheel speed of 850 r/min. With these, the qualified rate of seeding spacing was 95.98%, the miss seeding rate was 0.36%, and the coefficient of variation of seeding spacing was 15.58%.

$$\begin{cases} \max Q \\ \min C \\ s.t. \begin{cases} 30\text{r/min} < X_1 < 100\text{r/min} \\ 50\text{mm} < X_2 < 66\text{mm} \\ 550\text{r/min} < X_3 < 850\text{r/min} \end{cases} \end{cases} \quad (20)$$

Validation experiment

The working process of the seed delivery device with a rotating brush wheel was captured by the high-speed camera, as shown in Figure 12. Under the constraint and guidance of flexible brush wheel and U-shaped slide track, the seeds moved closely to the tube wall, realizing the uniform, smooth and orderly delivery of seeds.

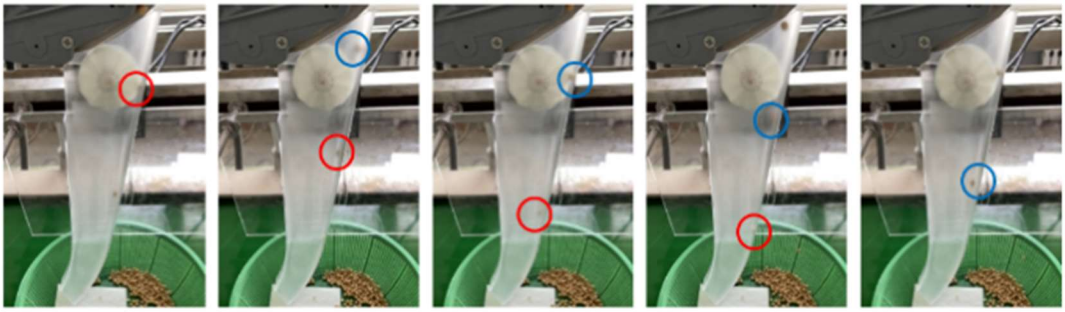

FIGURE 12. Seeding performance of seed delivery device with a rotating brush wheel.

During the validation experiment, the rotate speed of seed metering device was selected as 30, 45, 60, 75 and 90 r/min, and the corresponding forward speed was also given. The results were shown in Table 4.

TABLE 4. Results of the validation experiment.

Rotate speed of seed metering device/(r·min^{-1})	Forward speed/ (km·h^{-1})	Common seed delivery tube			Seed delivery device with a rotating brush wheel		
		Qualified rate of seeding spacing/%	Coefficient of variation of seeding spacing/%	Lateral deviation/ mm	Qualified rate of seeding spacing/%	Coefficient of variation of seeding spacing/%	Lateral deviation/ mm
30	6	94.40	15.2	11.9	96.62	13.23	6.7
44	8.8	90.09	17.46	15.6	95.29	14.12	8.9
60	12	82.74	24.13	16.7	92.14	16.62	9.7
75	15	76.07	28.47	23.6	87.02	17.25	13.3
90	18	68.64	33.22	25.7	83.30	19.50	15.8

As shown in Table 4, with the increase of forward speed or rotate speed of seed metering device, the qualified rate of seeding spacing of two devices decreased significantly, and the coefficient of variation of seeding spacing and lateral deviation increased significantly. Under the same forward speed, the working performance of seed delivery device with a rotating brush wheel was obviously better than that of common seed delivery tube. At a lower speed (forward speed ≤9 km/h), the qualified rate of seeding spacing reached more than 90% for the two devices, and the lateral deviation was both small. At a high speed (forward speed of about 12 km/h), the seed delivery device with a rotating brush wheel still maintained a higher qualified rate of seeding spacing (92.14%), a lower coefficient of variation of seeding spacing (16.62%) and lateral deviation (9.7 mm). Compared with the common seed delivery tube, the qualified rate of seeding spacing increased by 11.36%, the coefficient of variation of seeding spacing and the lateral deviation decreased by 31.12 % and 41.92%, respectively. At a very high speed (forward speed ≥15 km/h), the seed delivery device with a rotating brush wheel could still perform well. At the forward speed of 18km/h, the qualified rate of seeding spacing was 83.3% for the seed delivery device with a rotating brush wheel, while the common seed delivery tube could not meet the industry standard (qualified rate of seeding spacing ≥75%) (Wang et al., 2020b). Therefore, the seed delivery device with a rotating brush wheel could improve the seeding accuracy, especially in the high speed operation, it could still maintain a good working performance.

CONCLUSIONS

(1) Through theoretical analysis of U-shaped groove seed tube and flexible brush wheel, the seed delivery device with a rotating brush wheel was designed, which reduced the collision and deviation of seeds in the seed tube and made seeds move closely to the tube wall, realizing the uniform, smooth and orderly delivery of seeds.

(2) With air-suction seed metering device as the carrier, the optimization experiment was carried out by quadratic-regression rotatable orthogonal design method in JPS-12 seeding performance test bench. The three main factors were the rotate speed of seed metering device, the brush wheel diameter and the brush wheel speed. The evaluation indexes were the qualified rate of seeding spacing, miss seeding rate and coefficient of variation of seeding spacing. The results showed that the optimal parameters were rotate speed of seed metering device of 30 r/min, brush wheel diameter of 66 mm and brush wheel speed of 850 r/min. With these, the qualified rate of seeding spacing was 95.98%, the miss seeding rate was 0.36%, and the coefficient of variation of seeding spacing was 15.58%.

(3) The verification experiment was carried out. The test results showed that the working performance of seed delivery device with a rotating brush wheel was obviously better than that of common seed delivery tube under the same forward speed. In high speed operation (forward speed ≥15 km/h), the seed delivery device with a rotating brush wheel could still maintain a good working performance.

ACKNOWLEDGMENTS

This work was supported by the National Natural Science Foundation of China (Grant No. 52005307) and the National Key Research and Development Program of China (Grant No. 2021YFD2000401).

REFERENCES

Chen X, Zhong L (2012) Design and test on belt-type seed delivery of air-suction metering device. Transactions of the Chinese Society of Agricultural Engineering 28(22): 8-15. DOI: https: //doi.org /10.3969/j.issn.1002-6819.2012.22.002

Hou S, Zou Z, Wei Z, Zhu Y, Chen H (2020) Design and experiment of flexible mechanical soybean precision seed-metering device. Transactions of the Chinese Society for Agricultural Machinery 51(10): 77-86+108. DOI: https://doi.org/10.6041/j.issn.1000-1298.2020.10.010

Jin X, Li Q, Zhao K, Zhao B, He Z, Qiu Z (2019) Development and test of an electric precision seeder for small-size vegetable seeds. International Journal of Agricultural and Biological Engineering 12(2): 75-81.

Kang J, Wen H, Wang S, Yan L (2015) Experimental study on impact of belt type conductor delivery on seeding uniformity. Journal of Chinese Agricultural Mechanization 36(5): 42-45. DOI: https://doi.org/10.13733/j.jcam.issn.2095-5553.2015.05.011

Kireev IM, Fsbsi R, Koval ZM (2019) Study of the distribution of seeds using a pneumatic precision drill assembly. Machinery and Equipment for Rural Area (6): 12-17.

Lei X, Liao Y, Cong J, Wang L, Zhang Q, Liao Q (2018) Parameter optimization and experiment of air-assisted centralized seed-metering device of direct seeding machine for rape and wheat. Transactions of the Chinese Society of Agricultural Engineering 34(12): 16-26. DOI: https://doi.org/10.11975/j.issn.1002-6819.2018.12.003

Li Y, Yang L, Zhang D, Cui T, Zhang K, Xie C, Yang R (2020) Analysis and test of linear seeding process of maize high speed precision metering device with air suction. Transactions of the Chinese Society of Agricultural Engineering 36(9): 26-35. DOI: https://doi.org/10.11975/j.issn.1002-6819.2020.09.003

Liao Y, Li C, Liao Q, Wang L (2020) Research progress of seed guiding technology and device of planter. Transactions of the Chinese Society for Agricultural Machinery 51(12): 1-14. DOI: https://doi.org/10.6041/j.issn.1000-1298.2020.12.001

Liu J, Zhang P, Liu F (2016) The Discrete Element Simulation Guide Tube Height Effects on Seeding Performance. Journal of Agricultural Mechanization Research 38(01): 12-16. DOI: https://doi.org/10.13427/j.cnki.njyi.2016.01.004

Liu Q (2017) Design and experiment of seed precise delivery mechanism for high-speed planter. PhD Thesis, China Agricultural University.

Nielsen SK, Munkholm LJ, Lamande M, Norremark M, Edwards GTC, Green O (2018) Seed drill depth control system for precision seeding. Computers and Electronics in Agriculture (144): 174-180.

Wang J, Tang H, Wang J, Li X, Huang H (2017) Optimization design and experiment on ripple surface type pickup finger of precision maize seed metering device. International Journal of Agriculture and Biological Engineering 10(1): 61-71.

Wang W, Diao P, Jia H, Chen Y (2020b) Design and experiment evaluation of furrow compaction device with opener for maize. International Journal of Agricultural and Biological Engineering 13(2): 123–131

Wang Y, Zhang W, Yan W, Qi B (2020a) Design and experiment of seed pressing device for precision seeder based on air flow assisted seed delivery. Transactions of the Chinese Society for Agricultural Machinery 51(10): 69-75. DOI: https://doi.org/10.6041/j.issn.1000-1298.2020.10.009

Yang L, Yan B, Zhang D, Zhang T, Wang Y, Cui T (2016) Research progress on precision planting technology of maize. Transactions of the Chinese Society for Agricultural Machinery 47(11): 38-48. DOI: https://doi.org/10.6041/j.issn.1000-1298.2016.11.006

Yu J, Ding Y, Liao Y, Cong J, Liao Q (2014) High-speed photography analysis of dropping trajectory on pneumatic metering device for rapeseed. Journal of Huazhong Agricultural University 33(3): 103-108. DOI: https://doi.org/10.13300/j.cnki.hnlkxb.2014.03.018

Yuan Y, Bai H, Fang X, Wang D, Zhou L, Niu K (2018) Research progress on maize seeding and its measurement and control technology. Transactions of the Chinese Society for Agricultural Machinery 49(9): 1-18. DOI: https://doi.org/10.6041/j.issn.1000-1298.2018.09.001

Zhao S, Chen J, Wang J, Chen J, Yang C, Yang Y (2018) Design and experiment on V-groove dialing round type guiding-seed device. Transactions of the Chinese Society for Agricultural Machinery 49(06): 146-158. DOI: https://doi.org/10.6041/j.issn.1000-1298.2018.06.017